SRTTU

JCARME
ISSN: 2228-7922

Journal of Computational and Applied Research
in Mechanical Engineering
Vol. 3, No. 1, pp. 41- 52, Autumn 2013
http://jcarme.srttu.edu



Investigation of electrokinetic mixing in 3D non-homogenous microchannels

J. Jamaati[a,*], H. Niazmand[b] and M. Renksizbulut[c]

[a] *Razi University, Department of Mechanical Engineering, Kermanshah, Iran*
[b] *Ferdowsi University of Mashhad, Department of Mechanical Engineering, Mashhad, Iran*
[c] *University of Waterloo, Department of Mechanical & Mechatronics Engineering, Waterloo, Canada*

Article info:
Received: 16/02/2012
Accepted: 21/03/2013
Online: 11/09/2013

Keywords:
Mixing,
Electroosmotic,
Helmholtz-Smoluchowski model,
Non-homogeneous.

Abstract
A numerical study of 3D electrokinetic flows through micromixers was performed. The micromixers considered here consisted of heterogeneous rectangular microchannels with prescribed patterns of zeta-potential at their walls. Numerical simulation of electroosmotic flows within heterogeneous channels requires solution of the Navier-Stokes, Ernest-Plank and species concentration equations. It is known that a 3D solution of these equations is computationally very intensive. Therefore, the well-known Helmholtz-Smoluchowski model is often used in numerical simulation of electroosmotic flows. According to 2D studies on electrokinetic mixing inside heterogeneous channels, existence of vortices within the flow field always increases mixing performance. Hence, it may be expected that similar observations pertain to mixing in 3D flows as well. However, investigations on 3D micromixers identified situations in which existence of vortices had little or no significant benefit to the mixing performance. Findings of the present work indicated degree of flow asymmetry as a key parameter for the mixing performance. Since 3D flows are more capable of developing asymmetrical flow patterns, they are expected to have better mixing performance than their 2D counterparts. The results presented here for different 3D cases showed that mixing performance could be improved significantly depending on the alignment of vortex plane relative to the mixing interface of the fluids. These observations confirmed that 2D simulations of mixing could not fully explain behavior of passive micromixers.

1. Introduction

Flows of liquids in micro-scale channels have attracted increasing interest recently due to fast developments in micro-fluidics and soft lithography. Flow and species transport in micro-scales typically experience laminar and often Stokes flow conditions (Re<1) even for

[*] *Corresponding author*
Email address: jafar_jamaati@yahoo.com

curved microchannels [1]. In the absence of turbulence, species mixing in micro-scales becomes inherently diffusion dominated and, therefore, requires very long mixing lengths and time scales. This issue creates significant challenges for designing micro-total-analysis systems or lab-on-chip devices [2-4], in which mixing macromolecules and biological species with very low mass diffusivities is often encountered.

Most efforts for the improvement of mixing efficiency have concentrated on reducing characteristic mixing length. In general, mixing in microchannels can be performed through passive or active mechanisms, for which different methods have been proposed [5]. Active mixers use external energy to enhance mixing efficiency and, thus, a higher mixing performance is typically achieved. However, the mechanical and electronic components required for active mixing can have significant disadvantages in some applications such as lab-on-chip devices. In contrast, passive mixing does not require external energy and the mixing process mainly depends on the channel geometry and physical properties of its walls. Different methods proposed for the augmentation of passive mixing mostly focus on creating chaotic advection. The parameters affecting chaotic mixing have been studied and effects of aspect ratio, channel folding and variable channel cross section have been also investigated [6, 7].

A careful design of micromixer geometry can effectively reduce mixing length such as in lamination micromixers where mixing length is reduced through lamination of the components [8]. Lamination mixing is mostly affected by inlet conditions of the mixing components. One advantage of lamination mixing is hydrodynamic focusing [9], which can be implemented in electroosmotic flows [10]. Also, compatible lamination micromixers have been designed for pressure-driven flows in which effective length for molecular diffusion is reduced to half as the fluid passes through the mixer [11].

It has been found that surface grooves [12] adjusted with suitable direction [13, 14] result in more hydrophobic surfaces with higher slip velocities adjacent to the walls suitable for chaotic mixing. The investigation of electroosmotic flows in heterogeneous microchannel (both analytically [15- 17] and numerically [18- 20]) has indicated that surface heterogeneities, especially in zeta-potential, results in flow patterns with circulation zones and subsequent breakdown of the vortices by any means creates chaotic mixing. Chaotic mixing occurs only in 2D transient flows [21, 22] or 3D flows [23].

In general, for the numerical study of electroosmotic flows through heterogeneous microchannels, it is necessary to find the electric potential field and solve the equations of ion transport along with the Navier-Stokes equations [24, 25]. Numerical solutions of this set of equations in 3D flows are clearly very intensive. Reasonably, it is possible to solve the electric field and ion distribution only in the region adjacent to the walls and solve the standard Navier-Stokes equations in the electrically neutral region away from the walls [26]. The well-known simplification for electroosmotic flows is to assume the similarity between electroosmotic flow field and the corresponding electric field. The validity of this assumption has been thoroughly analyzed [27, 28]. An important case of this theory leads to the Helmholtz-Smoluchowski (H-S) model in which effects of the EDL (Electric Double Layer) on the flow field are considered through slip boundary conditions at the walls.

Using recent advances in micro patterning of microchannels with electrical charges [29, 30], it is possible to design channels suitable for both pumping and mixing tasks [31]. Effects of zeta-potential on the mixing efficiency have been studied [17, 23] and its applications for mixing chambers have been investigated [32]. It is vital to devise a proper indicator for the assessment of mixing performance. For simple flows without circulation regions, it is reasonable to define a mixing indicator based on the variance of the concentration profiles at each cross section [6, 13 and 33]. Also, the entropy related to the concentration field can be used as a basis for determining mixing performance [34- 36].

Ignoring the flow field characteristics in defining a mixing indicator introduces some physically inconsistent oscillations into mixing indicators in the regions involving vortex structures [18, 22, 31, 36- 38]. Therefore, it is essential to define a proper indicator involving characteristics of both concentration and flow fields, which is done via weighted standard deviation of concentrations with the axial velocity profile as the weighting function [29].

In this paper, 3D mixing in electroosmotic flows through microchannels with heterogeneous patterns of zeta-potential was investigated using the H-S model. The assessment of mixing performance was carried out with a proper mixing indicator defined based on the weighted variance of concentrations at any cross section with a proper weighting function. To study electrokinetic mixing, three different zeta-potential patterns (patches) were devised for the mixing section of the channel while uniform zeta-potential was assumed for the rest of the channel to act as a pump, supplying the driving force when the channel was exposed to an axial electric field. Several values of the zeta-potential for the pumping section were also examined. Moreover, effects of positioning the proposed patches at the walls were investigated in detail.

2. Modeling electroosmotic flows

Geometry of the channel studied in the present work and location of the mixing section are shown in Fig. 1. The microchannel had total length of L=6H, width of W=H and height of H=5μm. The ratio of W/H was set at 1 intentionally, allowing for the study of patch location effects in the absence of any aspect ratio influences on the mixing performance. The mixing section located in the middle part of the microchannel had length of $L_2 = 2H$, which consisted of two pairs of chemically distinct patches with length $L_{patch} = H$ attached to the walls in parallel. The patches had equal zeta-potentials of $\zeta_M = 50\,mV$ that could be adjusted to be positive or negative. The channel sections before and after the mixing section, denoted by lengths L_1 and L_3, respectively, had equal lengths of $L_1 = L_3 = 2H$ and uniform wall zeta-potentials denoted by ζ_P. These two sections served as the electroosmotic pumps for moving the fluid through the microchannel.

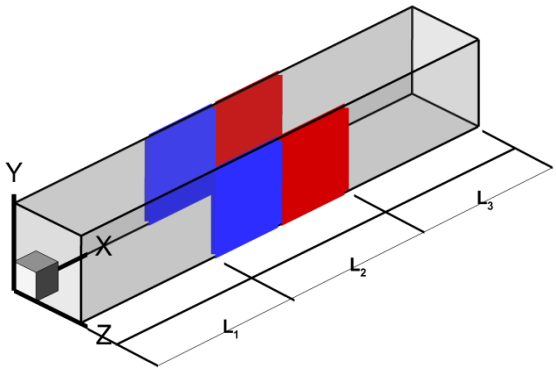


Fig. 1. The microchannel geometry and position of patches in the mixing section.

The governing equations for the flow field of electroosmotic flow are the continuity and Navier–Stokes equations:

$$\vec{\nabla}\cdot\vec{V} = 0 \tag{1}$$

$$\rho\left(\frac{\partial\vec{V}}{\partial t} + \left(\vec{V}\cdot\vec{\nabla}\right)\vec{V}\right) = -\vec{\nabla}p + \mu\nabla^2\vec{V} + \rho_e\vec{E} \tag{2}$$

where $\vec{V}$ is the velocity vector. The last term in the momentum equation is the body force due to electric field in which $\vec{E}$ is strength of electric field and ρ_e is density of free charges. For the general case, calculation of electric field and electrical charges requires solving ion transport equation, which is numerically expensive. An approximate approach is to use the well-known H-S model, in which effects of the electric force are considered via a prescribed slip velocity condition; in return, the body force is omitted from the Navier-Stokes equation.

In this model, the slip velocity at walls is a function of the external electric field E_0, the electrical permittivity of the solution ε, the reference EDL zeta-potential ζ_0, and the

viscosity of the fluid μ, such that $U_{EOF} = -\varepsilon\zeta_0 E_0 / \mu$. This equation is the well-known Helmholtz-Smoluchowski expression relating the electroosmotic velocity in the microchannel to the zeta-potential at the wall and the electric field applied. Here, the H-S model is adopted in performing 3D simulations of electrokinetic mixing in heterogeneous microchannels. Hence the governing equations of motion reduce to:

$$\rho\left(\frac{\partial \vec{V}}{\partial t} + (\vec{V}\cdot\vec{\nabla})\vec{V}\right) = -\vec{\nabla}p + \mu\nabla^2\vec{V} \quad (3)$$

the Eq. (3) is then subjected to slip boundary condition as below:

$$x = 0, L : \frac{\partial u}{\partial x} = 0 \;\&\; \frac{\partial v}{\partial x} = 0$$
$$y = 0, H \;: v = 0 \;\&\; u = -\varepsilon\zeta(x)E_0 / \mu \quad (4)$$

The concentration field is governed by the species convection–diffusion equation:

$$\rho\left(\frac{\partial C}{\partial t} + (\vec{V}\cdot\vec{\nabla})C\right) = D\nabla^2 C \quad (5)$$

where D is the diffusion coefficient and C is the concentration of the species. The inlet conditions for the above equation are:

$$x = 0 : C = \begin{cases} 0, & 0 < y/H < 0.5 \\ 1, & 0.5 < y/H < 1 \end{cases} \quad (6)$$

At all microchannel walls, the condition of zero mass flux is applied in the following form:

$$y = 0, H : \frac{\partial C}{\partial y} = 0 \quad (7)$$

A single flow domain was used with structured uniform mesh and two fluids had the same properties. The two fluids only differed in a scalar property which was concentration and the concentration equation similar to the heat equation was used to investigate the mixing.

3. Micromixer design

When a homogeneous microchannel with $\zeta_0 = -50\text{mV}$ at all walls is subjected to a uniform electric field with the intensity of $E_x = 29.7V / mm$, the induced slip velocity at the walls becomes $U_{EOF} = 1mm / s$, resulting in a uniform channel flow. Such a uniform laminar flow field typically has very poor mixing characteristics. However, it is possible to achieve highly non-uniform flows in microchannels by means of chemically distinct patches located at the walls, where adjustment of charges and electric field direction can result in a variety of complicated flow patterns. The heterogeneous micromixer channels studied here consisted of an initially uniform zeta-potential section subjected to a uniform electric field E_x (for fluid pumping purposes), followed by a mixing section where both zeta-potential and direction of the electric field were modified. This layout enabled construction of channels with a desired pattern of slip velocities at walls, dominantly axial in the pumping section but partly lateral in the mixing section. As stated before, the mixing section consisted of four uniform patches including two patches with $\zeta_0 = -50mV$ and two patches with $\zeta_0 = +50mV$. Three different arrangements could be considered in the mixing section with these sets of patches, which significantly affected the flow field in the microchannel. Figure 2 shows the corresponding streamlines of these patterns subjected to an electric field in the x direction. In case (a) of Fig. 2, at both upper and lower walls, the first patch had a positive zeta-potential of $\zeta_0 = +50mV$ while the second one had a negative zeta-potential of $\zeta_0 = -50mV$. Case (b) was similar to case (a); however, order of patches was reversed at the upper wall. Finally, in case (c), both negative patches were placed at the upper wall, which formed a double negative patch while both positive patches were placed at the lower wall. Other combinations could be imagined with these four patches, which included the mirror-image situations of the above cases and were not therefore considered. The colored areas in Fig. 2 indicate values of slip velocities at the

heterogeneous walls. Only the patched walls were shown here to have a better view of the interior flow field. The corresponding slip velocities of red, green and blue regions were $1mm/s$, $0.25mm/s$ and $-1mm/s$, respectively. For all the cases shown in Fig. 2, the electric field was applied in the x direction and, consequently, direction of slip velocities was also in the x direction. The flow field studied in Fig. 2 had a special characteristic. The pattern of zeta-potential at the wall was symmetric with regard to the mid-plane $(z=1/2)$, as demonstrated in this figure. Hence, obviously, all the streamline remained in this plane and no fluid element moved across it. Also, no mixing happened via advection mechanism. However, mixing happened through the diffusion mechanism and that was the reason concentrations changed along these streamlines.

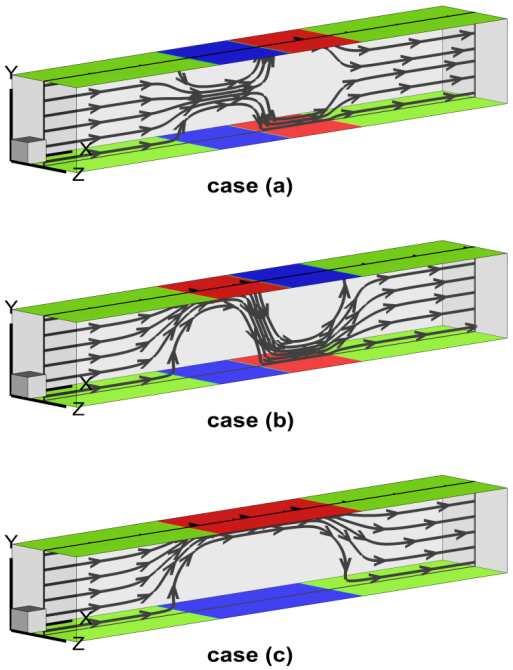


Fig. 2. Flow fields corresponding to three patch patterns considered in the mixing section.

Pressure and concentration fields of the flows shown in Fig. 2 are presented in right and left columns of Fig. 3, respectively. For these cases, values of zeta-potential in the pumping section were smaller than those in the mixing section. Hence, mixing characteristics of microchannels were dominant to the pumping characteristics and, in a short distance after the microchannel inlet, a perfect mixing was achieved as can be observed in the right columns of Fig. 3. The corresponding pressure fields are shown in left columns of Fig. 3. It is important to note that the flows studied here were all basically wall-driven and the pressure field was the result of fluid movement which was smooth everywhere in the microchannel unless in the patch intersections. In these regions, a significant pressure was observed, as demonstrated in the left columns of Fig. 3.

In 3D micromixers, electric field could be applied in three different directions. Therefore, even with a fixed pattern of charges at the walls, different flow fields could be generated depending on direction of the applied electric field over the patch areas and the plane on which the patch was located. In Fig. 4, the streamlines and slip velocity contours of all possible configurations corresponding to a prescribed charge pattern (pattern of case (a) considered here) are shown. In Figs. 4(i) and 4(ii), the induced slip velocities are in the x direction. In case (i), the prescribed pattern was applied at both upper and lower walls, characterized as $x-z$ planes while, in case (ii), the pattern was applied at the front and rear walls, denoted as $x-y$ planes. To have a better view of the flow patterns, the stream lines were shown only on the plane located at $z=W/2$. Later, the importance of this plane in mixing performance will be discussed. In cases (i) and (ii), the contours of u (x component of velocity) were shown in the planes of the patches. For both cases, the slip velocities on the patches were in the x direction. However, it can be seen that the corresponding flow patterns were considerably different due to the change in the plane, on which the patch was located. In case (iii), the patches were located at the front and rear walls

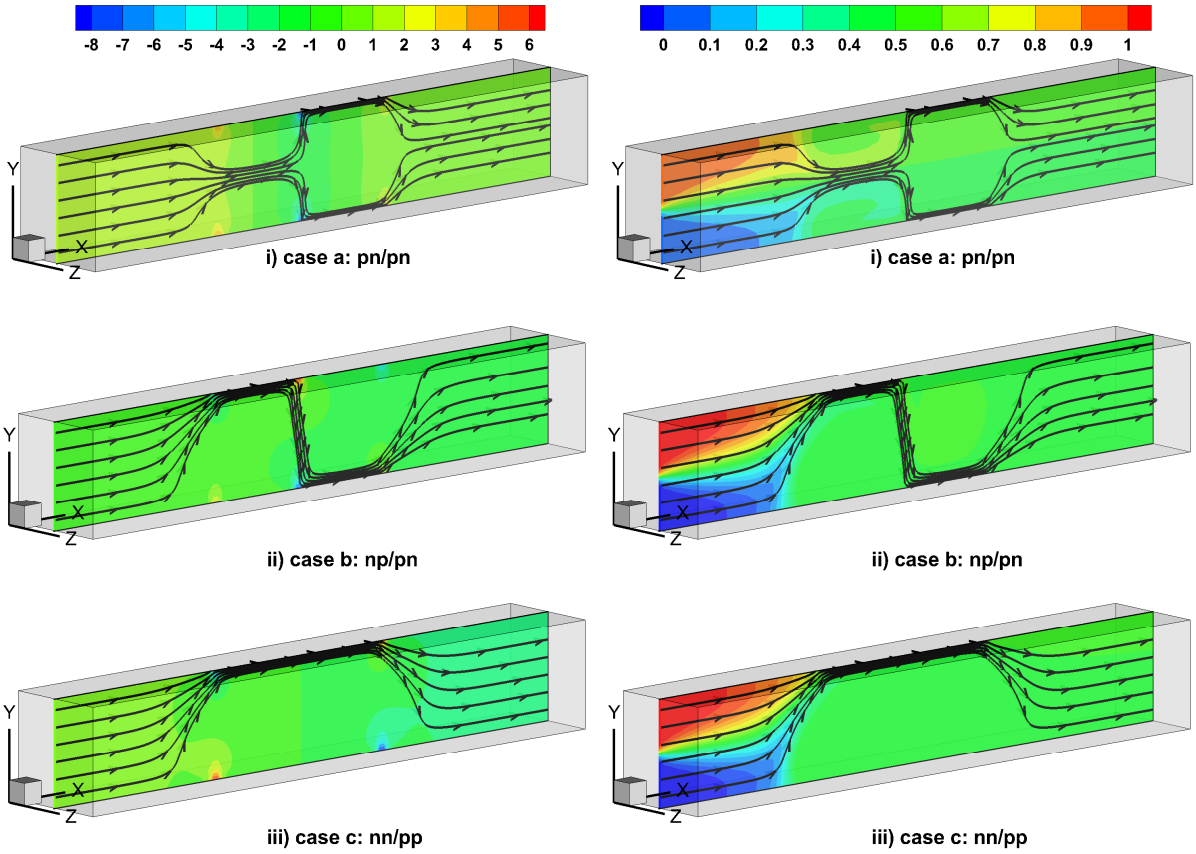


Fig. 3. pressure field (left) and concentration field (right) corresponding to flows of Fig. 2.

similar to case (i). However, the applied electric field in the patched areas was in the y direction. Hence, the induced velocities were formed in the y direction on the patches and the illustrated contours corresponded to the v component of the velocity vector. Finally in case (iv), the slip velocities on the patches were in the z direction and the contours of the w component of the velocity vector were demonstrated.

4. Numerical method and validation

To numerically solve the governing equations, the SIMPLEC algorithm was used for the pressure–velocity coupling with collocated variables in a uniform structured grid. In order to validate the numerical procedure, flow fields of different 2D electroosmotic flows inside heterogeneous microchannels with $L = 30H$ were simulated and verified by the analytical solution presented in [17]. Verification was performed for the most complicated flow pattern including some singular points that were numerically hard to capture. The prescribed function of slip velocities at upper and lower walls could be found in [17]. A comparison of the numerical and analytical flow fields is shown in Fig. 5 for a channel with height of $h = 2H$ and length of $L = 60H$. As can be seen, the analytical flow pattern was reasonably well predicted by the present numerical scheme. A grid study was performed for the independence of the mesh and it was concluded that a grid of $121 \times 21 \times 21$ was better to be used for calculation of the mixing performances. The numerical iteration was performed until all the relative residuals were smaller than 10^{-16}.

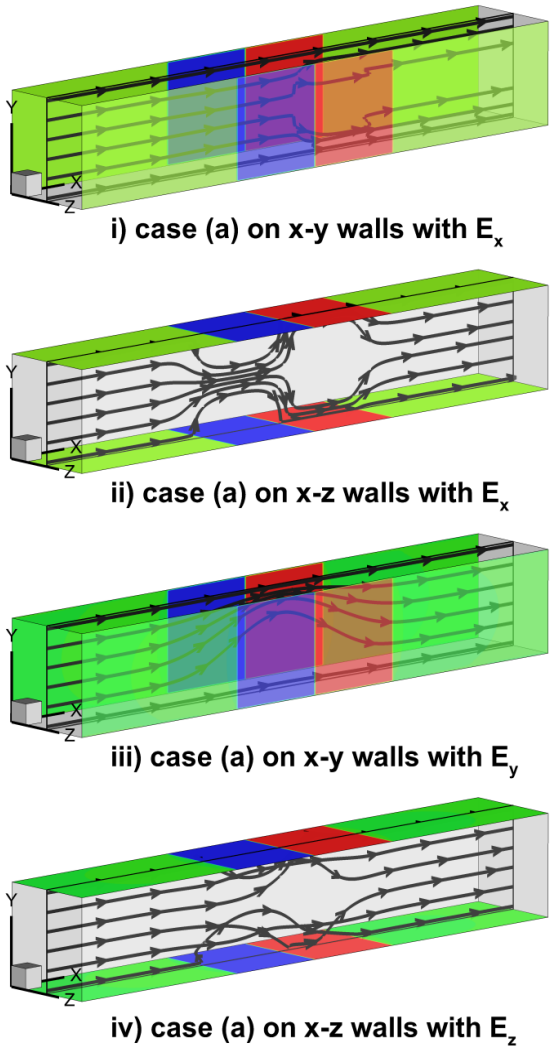


Fig. 4. Effects of plane of the patch and direction of the applied electric field over the patched areas.

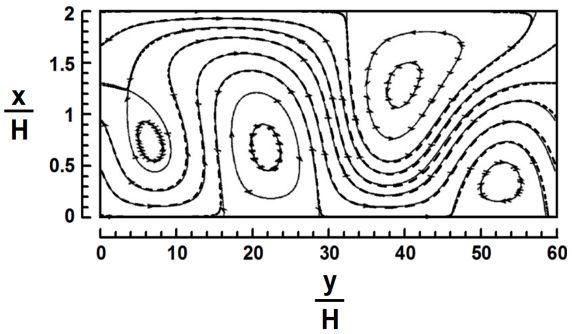


Fig. 5. Comparison of the present numerical results (dash lines) with the analytical solution of [17] (solid lines).

5. Results and discussion

This study investigated electroosmotic flow of a liquid with a relative dielectric constant $\varepsilon_r = 78.5$, density $\rho = 1000 kg/m^3$ and viscosity $\mu = 1.025 \times 10^{-3} Pa \cdot s$ in a microchannel with $H = 5\mu m$, $W = 5\mu m$ and $L = 30\mu m$. Magnitude of the applied electric field was $E_x = 29.7 V/mm$ and a uniform zeta-potential was considered at all channel walls, except in the mixing section, in which the zeta-potentials were adjusted according to the patterns indicated earlier. For a pure electroosmotic flow, the mass flow rate through the microchannel was related to the net charge at the microchannel walls. Here, the mixing section had no effect on the mass flow rate because net charge of the mixing section was intentionally set to zero. Hence, value of the zeta-potential in the homogeneous parts of the microchannel controlled the mass flow rate, which was also the reason for referring to this section as the pumping section. Figure 6 shows streamlines and concentration fields corresponding to case (b) in Fig. 2 for two different mass flow rates adjusted by the zeta-potential in the pumping section. Two fluids with the same physical properties but different concentrations of a scalar property entered the microchannel at $x = 0$. This illustration of the concentration field was limited to the region in which $0.3 < C(x, y, z) < 0.7$ in order to allow for a better 3D view of the mixing quality within the channel.

In Fig. 6(i), ratio of the zeta-potential in the pumping sections, i.e. sections before and after the mixing section, to the one in the mixing section was $\zeta_P / \zeta_M = 0.25$, which was quite small. In this condition, the associated Reynolds number was also very small and the slow motion of the fluid layers along the channel provided sufficient residence time for the occurrence of mixing. It can be seen that initially diffusion mechanism formed a narrow mixed layer

adjacent to the interface of the two fluids, which was then expanded because of advection effects in the mixing section where lateral velocities were significant. In case (ii) of Fig. 6, the pumping effect increased due to the increase in the value of ζ_P, which was accompanied by stronger advection effects. Therefore, thickness of the initially diffused layer was smaller and, at the same time, effects of secondary flows formed in the mixing section were weakened as compared to the main flow. Hence, benefits of advective mixing became limited and mixing developed in a narrow strip adjacent to the fluid interface.

In order to study the mixing performance quantitatively, it is important to introduce a proper mixing parameter. Previous studies indicate that a weighted standard deviation (where the velocity profile is used as the weighting function) is suitable to quantify the mixing performance in these complex flows with circulation zones. Using a weighted standard deviation, the mixing performance at any location in the channel can be evaluated using:

$$\varepsilon_M(x) = \frac{1-\sigma_W(x)}{1-\sigma_{W,min}} \quad (8)$$

where $\sigma_{W,min}$ is a reference value of the weighted standard deviation which is equal to 0 for the present problem and $\sigma_W(x)$ is the local value of the weighted standard deviation defined as:

$$[\sigma_W(x)]^2 = \frac{\int_0^W \int_0^H u(x,y,z)\left(C(x,y,z)-C_m\right)^2 dydz}{\int_0^W \int_0^H u(x,y,z)dydz} \quad (9)$$

where C_m is average concentration at any cross section.

Figure 7 shows mixing performance of the cases shown in Fig. 2 for two different mass flow rates mentioned earlier. Also, the corresponding mixing performance of homogeneous microchannels without patches was plotted for reference. This figure shows that mixing efficiencies of patterned channels before the mixing section were almost identical to those of homogeneous microchannels; however, considerable enhancement occurred in the mixing section of heterogeneous channels. Consistent with Fig. 5, for the low pumping power case denoted by $\zeta_P / \zeta_M = 0.25$, greater augmentation in the mixing performance was obtained using the heterogeneous microchannel. The best performance occurred for case (b), in which the highest asymmetry existed in the mixing section. The mixing performances of cases (b) and (c) were quite similar in the first half of the mixing section while, in the second half, case (b) provided a higher mixing effect due to greater asymmetry in its charge pattern.

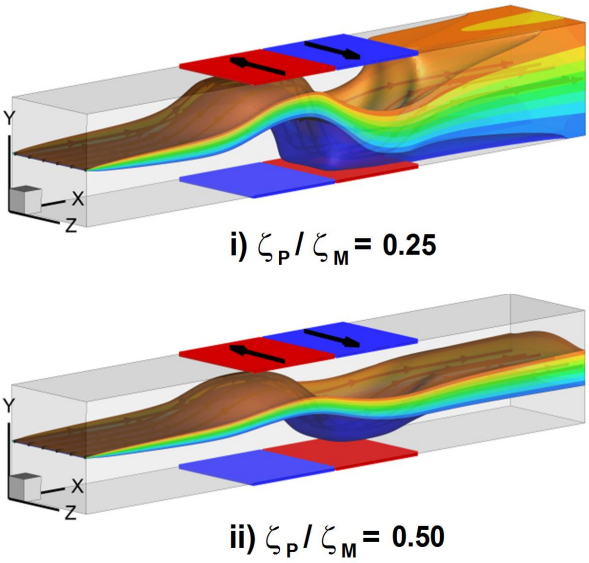


Fig. 6. Qualitative comparison of mixing in different mass flow rates controlled by the zeta-potential ratio.

Figure 8 shows possible combination of electric field directions and orientation of the patch planes for case (a). As stated before, four different configurations existed for each pattern in the mixing section. Again, the mixing performance was much higher for the lower pumping case of $\zeta_P / \zeta_M = 0.25$. For both cases (i) and (ii), the electric field was in the x direction.

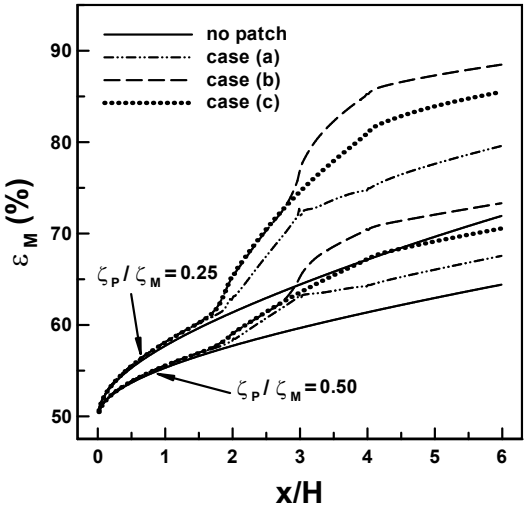


Fig. 7. Mixing performance of micromixers defined in Fig. 2 for two different values of the zeta-potential ratio.

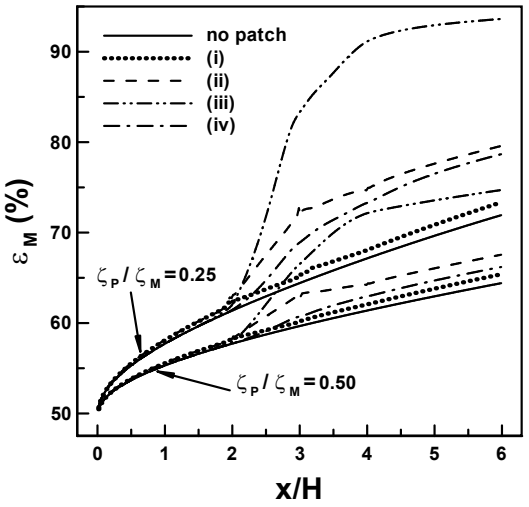


Fig. 8. Mixing performance of possible combinations of the electric field direction and the patch plane for case (a).

Case (i) had the poorest mixing performance because circulation plane of the vortex was parallel to the mixing interface. Consequently, interface of the two fluids experienced no significant folding or stretching due to vortices. The best mixing performance could be observed in case (iii). In this case, the interface experienced intense folding due to lateral motion induced by the doubled-patching in the mixing section.

It is obvious that, for a microchannel with specified length, the highest mixing efficiency occurred at the outlet of the channel. Therefore, value of the mixing efficiency at the end of the channel could be used as an indication of overall channel efficiency (ε_{Ch}) which can be used to compare mixing performance of different microchannels. According to Figs. 2 and 3, there were 12 different cases corresponding to combinations of patch arrangement and electric field direction.

Channel efficiencies of these cases were examined for $\zeta_P / \zeta_M = 0.25$. For this condition, efficiency of the homogeneous channel was 71.9%. The corresponding efficiencies of non-homogeneous microchannels are reported in Table 1.

Table 1. Mixing efficiencies (%) for different configurations of patches and directions of the electric field.

Electrical field direction	E_x	E_x	E_y	E_z
Patch planes	x-y	x-z	x-y	x-z
Case (a)	73.3	79.6	93.6	78.6
Case (b)	73.2	88.5	83.4	82.3
Case (c)	72.5	85.5	87.9	86.7

With an applied electric field in the x direction, it is observed in Table 1 that mixing performance was better when the patches were located in the $x-z$ planes rather than the $x-y$ planes. In both categories, the flows over the patches formed closed recirculation zones, which were in direct contrast to the axial velocity field and thus narrowed the effective main flow area leading to the increase in convective effects. The observation that patches in the $x-z$ plane produced greater channel efficiencies could be explained by referring to the circulation planes of the vortices For all the cases considered in the present work, the interface between the two fluids entering the microchannel coincided with the $y = 0.5$ plane, which was parallel to $x-z$ planes. Therefore, the vortices which cut through the interface were more effective in

enhancing the mixing performance. On the other hand, the vortices which circulated in parallel with interface had no significant effect on increasing mixing. Channel efficiencies of the cases with E_x in Table indicated that flow fields with interface-crossing vortices increased channel efficiency up to 16.6% while flows with vortices parallel to the interface only increased the channel efficiency by 1.4% at most.

The last two columns of Table 1 correspond to cases with lateral electric fields applied in the mixing section. First, the category microchannels with the electric field E_y applied in the y direction with patches located on $x-y$ planes should be considered. For this category, the vortices rigorously cut the interface plane near the microchannel walls. Hence, a great mixing performance was achieved. In the other category, i.e. cases identified with E_z and $x-z$ planes, the intersection of vortices and interface occurred away from the walls where the secondary flows were not as strong as they were near the walls. According to the data in Table 1, the best enhancement of mixing performance was obtained with the flow field of case (a) when the patches were located on $x-y$ planes and the applied electric field in the mixing section was in the y direction. For this case, channel efficiency was about 93.6% which showed 21.7% augmentation compared to the homogeneous microchannel. In case of the best mixing performance, mixing quality could be illustrated by means of a group of particle tracks in Fig. 9.

6. Conclusions

In this work, 3D mixing efficiency of electroosmotic flows were investigated in microchannels with heterogeneous wall patterns of zeta-potential. The results showed that heterogeneous patterns significantly affected the mixing performance. Mixing augmentation could be achieved by means of stretching and folding fluid layers. For electroosmotic flows, the folding effects were dominant because stretching the fluid layer was related to velocity gradients and the slip conditions at the walls reduced velocity gradients due to the nature of electroosmotic flows. Therefore, folding fluid layers seemed to be more practical for the enhancement of mixing in such flows. Thus, it could be observed that alignment of the vortex plane relative to the mixing interface of the fluids was an effective parameter for assessing mixing performance. It could be inferred that interface-crossing vortices produced the best effect on mixing performance. The present study demonstrated that weighted variance of concentration could be used to define a consistent mixing indicator. It was also shown that values of mixing efficiencies were much larger in cases with lower mass flow rates because residence time of the fluid in the channel was longer and the secondary flows were stronger.

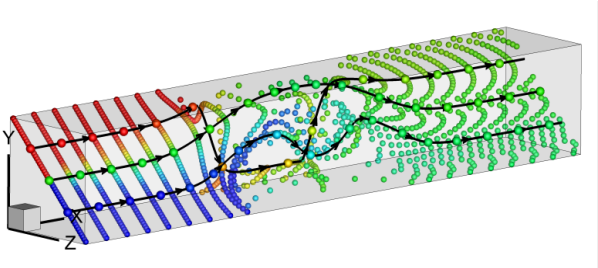


Fig. 9. Particle tracks for case (a) with E_y and patches on $x-y$ planes.

References

[1] J. K. Chen, W. J. Luo and R. J. Yang, "Electroosmotic flow driven by DC and AC electric fields in curved microchannels", *Jap. J. Appl. Phys.*, Vol. 45, pp. 7983-7990, (2006).

[2] G. M. Whitesides and A. D. Stroock, "Flexible methods for microfluidics", *Phys. Today*, Vol. 54, pp. 42-50, (2001).

[3] H. A. Stone, A. D. Stroock and A. Ajdari, "Engineering flows in small devices: microfluidics towards a lab-on-a-chip", *Annu. Rev. Fluid Mech.* Vol. 36, pp. 381-411, (2004).

[4] T. Vilkner, D. Janasek and A. Manz, "Micro total analysis systems", *Recent Developments Anal. Chem.*, Vol. 76, pp. 3373-3386, (2004).

[5] C. C. Chang and R. J. Yang, "Electrokinetic mixing in Microfluidic systems", *Microfluid Nanofluid*, Vol. 3, pp. 501-525, (2007).

[6] J. M. Chen, T. L. Horng and W.Y. Tan, "Analysis and measurements of mixing in pressure-driven microchannel flow", *Microfluid Nanofluid*, Vol. 2, pp. 455-469, (2006).

[7] D. P. J. Barz, H. F. Zadeh and P. Ehrhard, "3D simulations and experiments of flow in a folded microchannel", *PAMM Proc. Appl. Math. Mech.*, Vol. 6, pp. 559-560, (2006).

[8] S. H. Wong, M. C. L. Ward and C. W. Wharton, "Micro T-mixer as a rapid mixing micromixer", *Sensors Actuators B*, Vol. 100, pp. 365-385, (2004).

[9] J. B. Knight, A. Vishwanath, J. P. Brody and R. H. Austin, "Hydrodynamic focusing on a silicon chip: mixing nanoliters in microseconds", *Physical Review Lett.*, Vol. 80, pp. 3863-3866, (1998).

[10] R. J. Yang, C. C. Chang, S. B. Huang and G. B. Lee, "A new focusing model and switching approach for electrokinetic flow inside microchannels", *Micromech Microeng*, Vol. 15, pp. 2141-2148, (2005).

[11] S. Hardt, H. Pennemann and F. Schönfeld, "Theoretical and experimental characterization of a low-Reynolds number split and recombine mixer", *Microfluid Nanofluid*, Vol. 2, pp. 237-248, (2006).

[12] H. Aref, "Stirring by chaotic advection", *J. Fluid Mechanics*, Vol. 143, pp. 1-21, (1984).

[13] J. Ou, G. R. Moss and J. P. Rothstein, "Enhanced mixing in laminar flows using ultrahydrophobic surfaces", *Physical Review E*, Vol. 76, 016304 , (2007).

[14] P. B. Howell Jr, D. R. Mott, F. S. Ligler, J. P. Golden, C. R. Kaplan and E. S. Oran, "A combinatorial approach to microfluidic Mixing", *J. Micromech. Microeng.*, Vol. 18, pp. 115019-115026, (2008).

[15] J. Zhang, G. He and F. Liu, "Electro-osmotic flow and mixing in heterogeneous microchannels", *Physical Review E*, Vol. 73, pp. 056305-056312, (2006).

[16] Y. K. Lee, L. M. Lee, W. L. W. Hau and Y. Zohar, "Two-dimensional analysis of electrokinetically driven out-of-plane vortices in a microchannel liquid flow using patterned surface charge", *MEMS*, Vol. 16, pp. 58-67, (2007).

[17] K. Horiuchi, P. Dutta, and C. F. Ivory, "Electroosmosis with step changes in zeta-potential in microchannels", *AIChE*, Vol. 53, pp. 2521-2533, (2007).

[18] D. Erickson, and D. Li, "Influence of Surface Heterogeneity on Electrokinetically Driven Microfluidic Mixing", *Langmuir*, Vol. 18, pp. 1883-1892, (2002).

[19] K. Fushinobu, and M. Nakata, "An experimental and numerical study of a liquid mixing device for Microsystems", *Trans. ASME J. Electronic Packaging*, Vol. 127, pp. 141-146, (2005).

[20] L. M. Lee, W. L. W. Hau, Y. K. Lee and Y. Zohar, "In-plane vortex flow in microchannels generated by electroosmosis with patterned surface charge", *J Micromech. Microeng.*, Vol. 16, pp. 17-26, (2006).

[21] S. Qian and H. H. Bau, "A chaotic electroosmotic stirrer", *Anal. Chem.*, Vol. 74, pp. 3616-3625, (2002).

[22] C. K. Chen, and C. C. Cho, "Electrokinetically driven flow mixing utilizing chaotic electric fields", *Microfluid Nanofluid*, Vol. 5, pp. 785-793, (2008).

[23] C. C. Chang, and R. J. Yang, "A particle tracking method for analyzing chaotic electroosmotic flow mixing in 3-D microchannels with patterned charged

surfaces", *J Micromech. Microeng.*, Vol. 16, pp. 1453-1462, (2006).

[24] S. A. Mirbozorgi, H. Niazmand and M. Renksizbulut, "Electro-osmotic flow in reservoir-connected flat microchannel with non-uniform zeta-potential", *J. Fluids Engineering, Transactions of the ASME*, Vol. 128, No. 6, pp. 1133-1143, (2006).

[25] J. C. Ramirez and A. T. Conlisk, "Formation of vortices near abrupt nano-channel height changes in electro-osmotic flow of aqueous solutions", *Biomed Microdevices*, Vol. 8, pp. 235-330, (2006).

[26] I. Meisel and P. Ehrhard, "Electrically excited (electroosmotic) flows in microchannels for mixing applications", *European Journal of Mechanics B/Fluids*, Vol. 25, pp. 491-504, (2006).

[27] E. B. Cummings, S. K. Griffiths, R. H. Nilson and P. H. Paul, "Conditions for similitude between the fluid velocity and electric field in electroosmotic flow", *Anal. Chem.*, Vol. 72, pp. 2526-2532, (2000).

[28] J. G. Santiago, "Electroosmotic flows in microchannels with finite inertial and pressure forces", *Anal. Chem.*, Vol. 73, pp. 2353-2365, (2001).

[29] A. D. Stroock, M. Weck, D. T. Chiu, W. T. S. Huck, P. J. A. Kenis, R. F. Ismagilov and G. M. Whitesides, "Patterning electro-osmotic flow with patterned surface charge", *Physical Review Letters*, Vol. 84, No. 15, pp. 3314-3317, (2000).

[30] J. Park and B. Kim, "3D micro patterning on a concave substrate for creating the replica of a cylindrical PDMS stamp", *Microelectronic Engineering*, Vol. 98, pp. 540-543, (2012).

[31] N. Loucaides, A. Ramos and G. E. Georghiou, "Configurable AC electroosmotic pumping and mixing", *Microelectronic Engineering*, Vol. 90, pp. 47-50, (2012).

[32] J. R. Pacheco, A. Pacheco-Vega and K. P. Chen, "Mixing-dynamics of a passive scalar in a three-dimensional microchannel", *Int. J Heat and Mass Trans.*, Vol. 54, pp. 959-966, (2011).

[33] C. Simonnet and A. Groisman, "Chaotic mixing in a steady flow in a microchannel", *Physical Review Letters*, Vol. 94, pp. 134501- 134504, (2005).

[34] M. Camesasca, I. Manas-Zloczower and M. Kaufman, "Entropic characterization of mixing in microchannels", *J. Micromech. Microeng.*, Vol. 15, pp. 2038-2044, (2005).

[35] T. G. Kang and T. H. Kwon, "Mixing analysis of chaotic micromixers", *J. Micromech. Microeng.*, Vol. 14, pp. 891-899, (2004).

[36] N. S. Lynn, C. S. Henry and D. S. Dandy, "Microfluidic mixing via transverse electrokinetic effects in a planar microchannel", *Microfluid Nanofluid*, Vol. 5, pp. 493-505, (2008).

[37] D. Wang, J. L. Summers and P. H. Gaskell, "Modeling of electrokinetically driven mixing flow in microchannels with patterned blocks", *Computers and Mathematics with Applications*, Vol. 55, No. 7, pp. 1601-1610, (2008).

[38] C. C. Chang and R. J. Yang, "Computational analysis of electrokinetically driven flow mixing in microchannels with patterned blocks", *J. Micromech. Microeng.*, Vol. 14, No. 4, pp. 550-558, (2004).